

# Comparison of metal–amino acid interaction in Phe–Ag and Tyr–Ag complexes by spectroscopic measurements

Achintya Singha<sup>a</sup>, Swagata Dasgupta<sup>b</sup>, Anushree Roy<sup>a,\*</sup>

<sup>a</sup> Department of Physics, Indian Institute of Technology, Kharagpur 721302, India

<sup>b</sup> Department of Chemistry, Indian Institute of Technology, Kharagpur 721302, India

Received 5 September 2005; received in revised form 7 November 2005; accepted 15 November 2005

Available online 27 December 2005

## Abstract

In this article, we have compared the metal–amino acid interactions in Tyr–Ag and Phe–Ag complexes through pH dependent SERS measurements. By analyzing the variation in relative intensities of SERS bands with the pH of the amino acid solution, we have obtained the orientation and conformation of the amino acid molecules on the Ag surface. The results obtained from our experimental studies are supported by the energy minimized structures and the observed charge distributions in different terminals of the molecules. This, in a way, shows that SERS measurements not only exhibit the interaction of the amino acid molecules with Ag clusters but also demonstrate their orientation around it. We have addressed a long standing query on whether the amine group is directly attached to the Ag surface along with the carboxylate group and  $\pi$ -electrons in these systems. In addition, pH dependent optical absorption and transmission electron microscopy measurements have been performed to understand the required conditions for the appearance of the SERS spectra in the light of the aggregation of metal particles and the number of hot sites in the sol. Our results confirm that the formation of hot sites in the sol plays a direct role in forming a stable Ag–ligand complex. Furthermore, the interaction kinetics of metal–amino acid complexes have been analyzed via both Raman and absorption measurements.

© 2005 Elsevier B.V. All rights reserved.

**Keywords:** Metal–amino acid interaction; SERS; Optical absorption

## 1. Introduction

Spectroscopic studies of amino acids adsorbed on metal surfaces are important because they can provide an insight into the nature of metal–biopolymer interactions [1–5]. A number of articles have shown that amino acids with small side chains, for example, Glycine (Gly), Alanine (Ala), interact with metal colloids through both the amine and carboxylate terminals [2]. On the other hand, for Phenylalanine (Phe), Tyrosine (Tyr), Tryptophan (Trp), Histidine (His), Leucine (Leu), Glutamic acid (Glu), and Aspartic acid (Asp), the adsorption occurs through the carboxylate group. However, no conclusion is drawn regarding the amine–silver interaction [2,3].

Surface enhanced Raman scattering (SERS) is an extremely sensitive technique for monitoring the adsorption of species of very low concentration and for characterizing the structure and orientation of the adsorbed species on the rough metal surface

[6]. Nonresonance SERS is primarily sensitive to the species attached to the metal surface or present within a few angstroms of the metal–dielectric interface. Both electromagnetic field and adsorbate–surface chemical interactions are responsible for Raman signal enhancement. The ‘surface selection rules’ and the SERS intensity of a particular Raman band determine the average orientation of functional groups of the adsorbates on the metal surface [2]. In conjunction with optical absorption measurements it has been shown that the single metal cation does not exhibit any SERS effect. Complexation with an organic substance is necessary for signal enhancement [7]. The colloid activation by chemical treatment brings the primary metal particles close together building up ‘hot sites’ that are SERS active in an electromagnetic field of visible wavelength. ‘Hot sites’ are located at interstitial positions between metal particles and the number of such position scale with the number of particles. In the second step, the activating molecules of very low concentration are bound to the metal surface and form the complex [7]. Despite well-documented limitations, the spectral ‘richness’ in SERS arises not only from the inherent sensitivity

\* Corresponding author.

E-mail address: [anushree@phy.iitkgp.ernet.in](mailto:anushree@phy.iitkgp.ernet.in) (A. Roy).

of the process, but also from the ability of this technique to determine the interactions in the metal–adsorbate complex and the relative orientation and conformation of the adsorbed molecules on the metal surface.

The structural difference between Phe and Tyr is in the presence of only one –OH group in the *para* position of the aromatic ring in the latter [Fig. 1]. In solution, depending on the pH values [ $pK_1=2.58$  and  $pK_2=9.24$ ] the majority of Phe molecules assume the structural forms shown as species I–III in Fig. 1. Similarly, the structural forms of the majority of Tyr molecules in solution with different pH values [ $pK_1=2.20$ ,  $pK_2=9.11$  and  $pK_3=10.07$  (due to the side chain)] are shown as species I–IV in Fig. 1. In the sol, Ag particles are in the ionic  $Ag^+$  state because of its low oxidation potential. The electrostatic interaction between the above species of amino acid molecules with positively charged Ag particles in solution is one of the crucial factors for the SERS effect [8]. The structure of the molecules also plays an important role in determining the intensities of different SERS bands. Thus, a pH dependent study of SERS spectra with a comparison between the results for Phe and Tyr is expected to determine the metal–amino acid interaction and orientation of the adsorbed species on the metal surface.

The SERS spectra of Phe and Tyr adsorbed on Silver (Ag) colloids are available in the literature [3,9]. We find that though the structure of these molecules are very similar (as mentioned above), their SERS spectra are widely different. To understand

the interaction of these amino acids with Ag colloids we have studied the pH dependent optical absorption and SERS spectra of both Phe–Ag and Tyr–Ag complexes. From the relative change in intensities of the vibrational bands in SERS spectra we have compared the interaction, conformation and the orientation of these molecules on Ag particles. Section 2 covers the sample preparation techniques, which we have followed, and other details regarding the instruments, which we have used for various measurements. In Section 3, we have compared the possible surface geometry of the adsorbed Phe and Tyr on the surface of the Ag particles via pH dependent SERS measurements. Our conjecture from these experimental observations has been further supported by the surface geometry expected from the electrostatic interaction between  $Ag^+$  and Phe or Tyr, obtained from the estimated atomic charge distribution at the different terminals of the amino acid molecules. In this section we have also shown the role of formation of hot sites to exhibit SERS spectra for metal–amino acid complex through simultaneous pH dependent optical absorption and SERS measurements. The interaction kinetics between the adsorbate and Ag colloids has been discussed in Section 4. Finally, in Section 5 we have summarized our results with a few concluding remarks.

## 2. Materials and methods

Silver nitrate ( $AgNO_3$ ), sodium borohydride ( $NaBH_4$ ), sodium hydroxide (NaOH), and hydrochloric acid (HCl) of

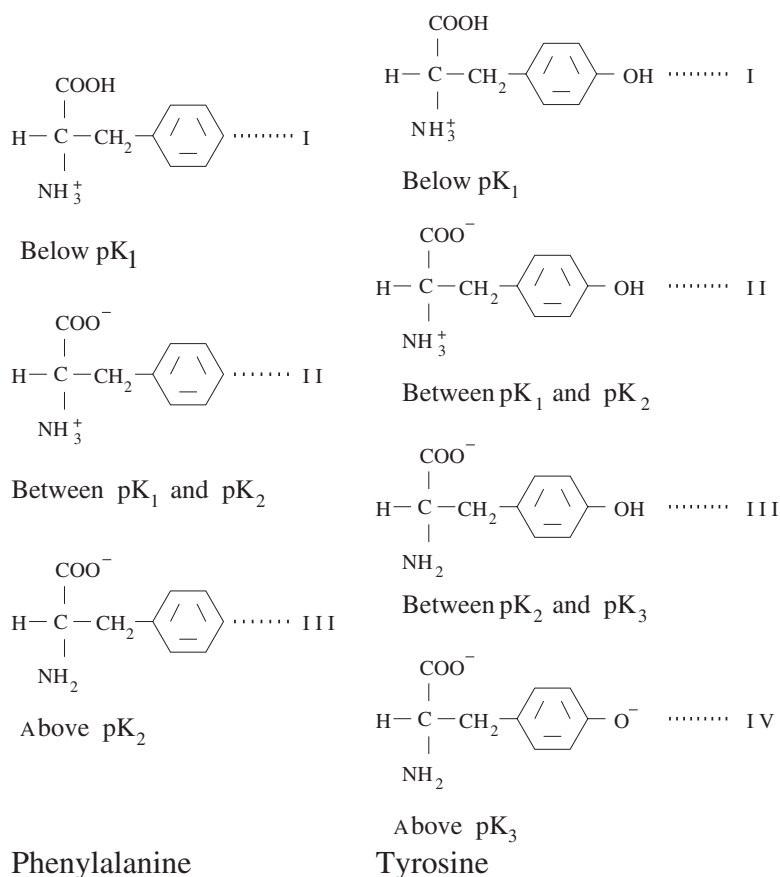


Fig. 1. Different ionic species of Phe and Tyr at different pH values.

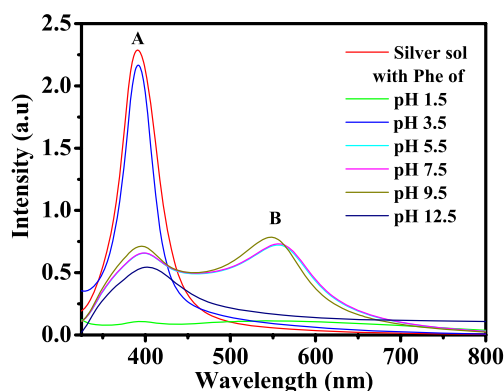


Fig. 2. Absorption spectra of Phe–Ag mixture at different pH values.

analytical reagent grade (SRL, India) were used to prepare the Ag sol and to maintain the pH of the solutions. Amino acids were also obtained from the above company. A colloidal silver solution was prepared in deionized water according to the method described by Creighton et al. [10]. This method essentially uses the reduction of  $10^{-3}$  M  $\text{AgNO}_3$  by an excess amount of  $10^{-3}$  M  $\text{NaBH}_4$ .  $10^{-3}$  M  $\text{AgNO}_3$  was added dropwise to  $10^{-3}$  M  $\text{NaBH}_4$  (placed in an ice bath under quick stirring condition) maintaining a 1:3 volume ratio. Stirring for 20 min was necessary to stabilize the colloidal solution. Later, it was left at room temperature for approximately 1 h. The excess  $\text{NaBH}_4$  decomposed and the solution became transparent yellow in colour.  $10^{-3}$  M solution of Phe and Tyr were prepared in deionized water. The pH of the solution was adjusted by using 1 M HCl and 1 M NaOH. For SERS and optical absorption measurements Phe and Tyr solutions of different pH were added to the Ag sol (of pH value 7.86). For all experiments the volume ratio of Ag sol to amino acid solution was maintained at 9:1.

In this article, the quoted pH values of the solutions for all spectroscopic and transmission electron micrograph (TEM) measurements were measured for Phe/Tyr prior to their addition to the Ag sol. We found that when the amino acid residues were not in the zwitterionic form, there was no substantial change in the pH values of the Phe–Ag/Tyr–Ag sol from those of the initial Phe/Tyr solutions. In other words, for species I and III of Phe and species I and IV of Tyr in Fig. 1, the pH of Phe–Ag/Tyr–Ag sol was nearly same as that of the Phe/Tyr solution prior to addition. However, in the zwitterionic form of the Phe (Tyr), for an initial value of pH between 2.89 and 9.20 (between 2.70 and 9.71) the final pH of Phe–Ag (Tyr–Ag) sol changed to  $7.2 \pm 0.07$  ( $7.17 \pm 0.07$ ). It was also

noted that the final pH of the mixed sol did not stabilize even after 15–20 min.

Raman and SERS spectra were measured in back-scattering geometry using a 488 nm Argon ion laser as an excitation source. During measurements the samples were kept in a rectangular quartz cell. The optical pathlength within the sample was 1 cm. The spectrometer was equipped with a 1200 grooves/mm holographic grating, a holographic super-notch filter, and a Peltier cooled CCD detector. The laser power density on the samples was tuned to  $3 \times 10^4 \text{ W/m}^2$ . The data acquisition time for each Raman and SERS spectrum was 120 s. We have reported all Raman and SERS spectra of Phe after subtracting the broad background due to water in the range 1500–1800 and 2800–3200  $\text{cm}^{-1}$ . For 488 nm as excitation wavelength, the Raman spectrum of Tyr appears on its rising luminescence background. Raman spectra of Tyr are shown after subtracting this background. In this article, the reported Raman or SERS peak intensities are the peak heights after subtracting the above mentioned backgrounds.

UV–visible spectra were measured by Spectrascan UV 2600 (Chemito). All absorption spectra are recorded 2 min after addition of the amino acid to the sol. Samples for TEM were deposited onto 300 mesh copper TEM grids coated with 50 nm carbon films. The excess water was allowed to evaporate in air. The grids were examined in JEOL 2010 microscope with Ultra-High Resolution (UHR) microscope using a  $\text{LaB}_6$  filament operated at 200 kV.

The amino acid zwitterionic structures were drawn and energy minimized using SYBYL 6.92 (Tripos Inc., St. Louis USA). The structures were rendered in Pymol (Delano Scientific LLC, USA). The atomic charge distribution of the molecules has been estimated using the Gasteiger–Hückel method.

### 3. Adsorption of Phenylalanine (Phe) and Tyrosine (Tyr) on silver colloidal surface: optical absorption and SERS measurements

#### 3.1. Phenylalanine (Phe): results and discussion

The optical absorption spectra (OAS) of Phe at different pH in a colloidal solution of Ag are shown in Fig. 2. The Ag sol absorbs light at  $\lambda_{\text{max}} = 392 \text{ nm}$  (A) [Fig. 2]. This band is associated with the dipolar surface plasmon of small, single, spherical particles of Ag. Transmission electron micrograph (TEM) of Ag sol shows formation of well-dispersed spherical Ag particles [Fig. 3(a)]. The average diameter of the Ag

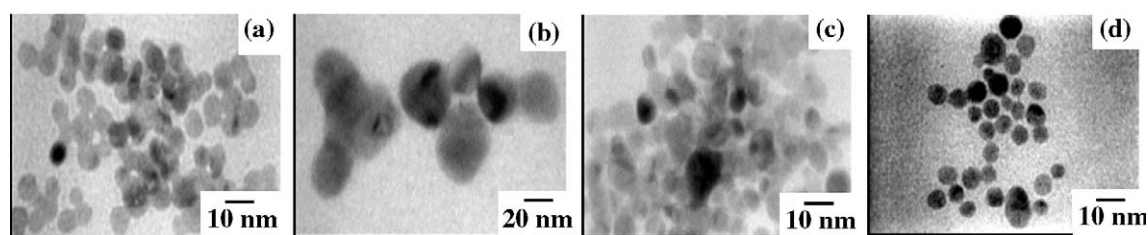


Fig. 3. Transmission electron micrograph of (a) Ag sol and Phe–Ag mixture at (b) pH 2 (c) pH 8, and (d) pH 11.

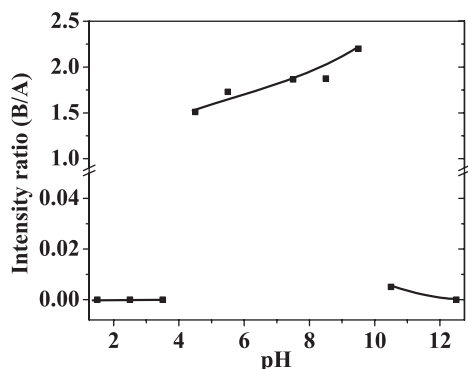


Fig. 4. Variation of intensity ratio of peak B to peak A in optical absorption spectra for Phe–Ag complex.

particles estimated from the  $\lambda_{\max}$  in OAS in Fig. 2 and TEM image in Fig. 3(a) is  $\sim 90$  Å.

Addition of Phe to the sol results in a decrease in intensity of peak A (due to the silver colloid without adsorbate), along with an appearance of a new band at around 550 nm (B) due to aggregated Ag particles. In Fig. 2 we have shown the change in the optical absorption spectrum of Ag sol with addition of Phe of pH varying from 1.5 to 12.5 in final Ag–Phe sol. The change in the ratio of intensity of peak B to that of peak A with variation in pH is shown in Fig. 4. The nature of aggregation of the silver particles, with addition of Phe of different pH, as obtained from TEM images, is shown in Fig. 3(b) to (d). Addition of Phe at a very low pH (below pH 2) to the Ag sol results in an immediate agglomeration and precipitation of Ag particles (not shown in the figure). One may also note the green curve in Fig. 2, where any signature of colloidal Ag particle is nearly absent. Between pH 2 and pH 3.5, the metal particles agglomerate appreciably. However, they are not big enough to precipitate immediately [Fig. 3(b) for pH 2]. For Phe with medium pH in Ag sol, one observes clustering of Ag particles in solution without much agglomeration or precipitation [Fig. 3(c) for pH 8 of Phe]. Addition of Phe at very high pH values (above 9) prohibits the clustering of Ag particles, which now spread out in solution [Fig. 3(d)].

In Fig. 5 we have shown the Raman spectrum of an aqueous Phe solution of 0.5 M (mentioned as Phe-C in the rest of the article) at pH 6.5 within the spectral window of 500–3200  $\text{cm}^{-1}$ . The assignments of bands in Phe-C,

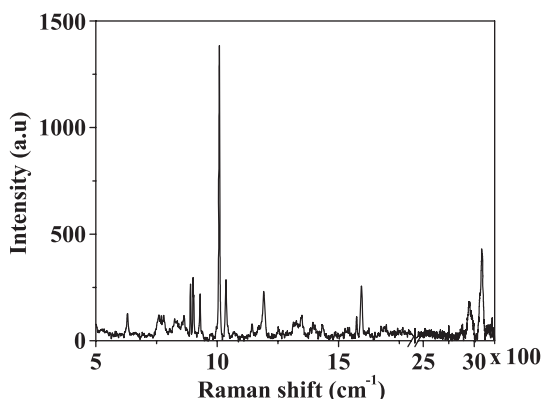


Fig. 5. Raman spectrum of Phe in solution at concentration 0.5 M.

Table 1

Assignment of vibrational bands for Phe-C (Raman spectrum) and Phe–Ag complex (SERS spectra)

Assignment	Phe-C ( $\text{cm}^{-1}$ )	SERS Phe ( $\text{cm}^{-1}$ )
Benzene ring breathing mode ( $\nu_1$ )	1008	1000 (★)
$\text{COO}^-$ rocking, wagging, bending	500–700	500–700
$\nu_{\text{C}-\text{C}}$ of benzene ring	901	–
C–H vibration in benzene ring	3080	3065 (X)
C– $\text{COO}^-$	929	936
CN	1036	1035
$\text{NH}_3^+$	1595	1582 (+)
CH	1251	1235
CH	2976	2915
$\text{COO}^-$	1413	1375 (\$)
$\text{CH}_2$ wagging	1332	–
$\text{CH}_2$ deformation	1400	–

In Fig. 6, the main SERS peaks are labelled by the marks given in parentheses.

summarized in Table 1, are based on the available Raman data for Phe [11,12]. The most intense band at 1008  $\text{cm}^{-1}$  has been assigned to the benzene ring breathing mode ( $\nu_1$ ). Other less intense but prominent bands appear at 901, 929, 1036, and 1595  $\text{cm}^{-1}$  due to  $\nu_{\text{C}-\text{C}}$ , C– $\text{COO}^-$ , CN and  $\text{NH}_3^+$  vibrations, respectively. The bands belonging to  $\nu_{\text{CH}}$ ,  $\nu_{\text{COO}^-}$ ,  $\text{CH}_2$  wagging, and  $\text{CH}_2$  deformation are weak and observed at 2976 (also at 1251), 1413, 1332 and 1400  $\text{cm}^{-1}$ , respectively.  $\text{COO}^-$  rocking, wagging, and bending modes appear between 500 and 700  $\text{cm}^{-1}$ . The feature at 3080  $\text{cm}^{-1}$  is due to the breathing motion of the hydrogen atoms in the benzene ring (C–H vibration).

SERS spectra (solid lines) of  $1 \times 10^{-3}$  M Phe, 2–3 orders of magnitude more dilute than the concentration typically required for nonresonant Raman scattering, with pH from 1.5 to 12.5 are shown in Fig. 6. We have recorded spectra of Phe–Ag complexes by changing the pH values by 1.0 unit over this range. However, in Fig. 6, we have shown a few characteristic spectra. SERS peak positions are also listed in Table 1. The Raman spectrum of aqueous Phe solution with the low concentration (0.001 M) at pH 7 is shown by the dotted line in the same figure.

To understand the interaction of the adsorbed species on the surface of Ag particles, we will make use of both SERS and

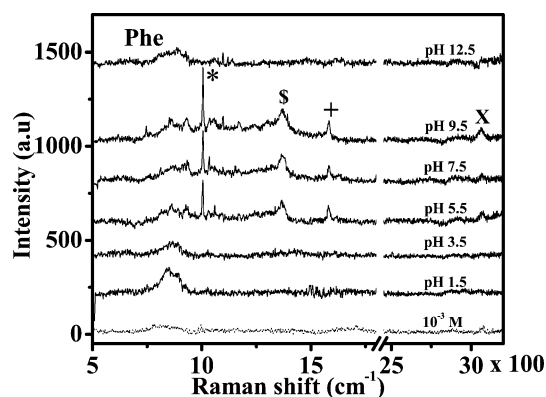


Fig. 6. Raman spectrum (dotted) of Phe and SERS spectra (solid lines) of Phe–Ag complex ( $1 \times 10^{-3}$  M) at different pH of Phe. The main features, which are to be noted, are at 1000 (★ mark), 1375 (\$ mark), 1582 (+ mark) and 3065  $\text{cm}^{-1}$  (X mark).



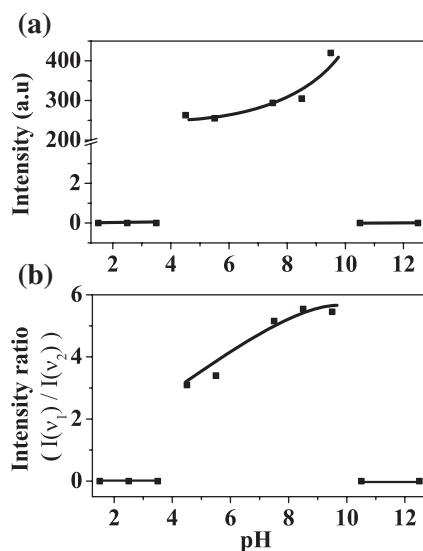


Fig. 7. Intensity variation of SERS bands at (a) 1000  $\text{cm}^{-1}$ , (b) intensity ratio  $I(v_1)/I(v_2)$  with pH variation from 1.5 to 12.5 for Phe–Ag complex.

absorption spectra. It is clear from Figs. 5 and 6 that intensities of the above mentioned vibrational modes change in SERS spectra with variation in pH. It is also interesting to note that below the pH value of 4.5 and above the pH value of 10 the SERS spectrum is extremely weak for the complex. As we mentioned before, upon addition of Phe of very low pH (below 3.5, value of  $\text{p}K_1=2.58$ ) the Ag particles agglomerate and then precipitate or form bigger particles [see Fig. 2 green curve and also Fig. 3(b)]. The high pH value (above 9.5,  $\text{p}K_2=9.24$ ) results in a spreading of Ag particles, as shown in Fig. 3(d). The slight red shifted broad navy blue spectrum for pH 12.5 in Fig. 2 indicates the presence of agglomerated Ag particles alone in the sol. Under both these conditions the number of hot sites decreases in solution, which in turn results in a decrease in the intensity of the SERS spectrum. In other words, the inefficient SERS is related to the failure of colloid activation due to insufficient complexation of Phe to the Ag surface. Intensities of the vibrational bands in SERS spectra are quite prominent, though of varying intensities, for the pH values ranging from 4.5 to 9.5. Thus, from Figs. 3 and 4, we conclude that for efficient SERS the aggregation of Ag colloidal particles (increase in intensity ratio of B to A in optical absorption spectra) plays an important role via the formation of hot sites.

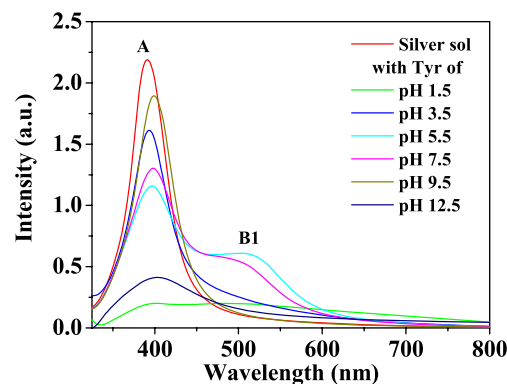


Fig. 9. Absorption spectra of Tyr–Ag mixture at different pH.

The SERS spectra at pH below 3.5, between 3.5 and 9.5, and above 9.5 should correspond to species I, II and III, respectively, shown in Fig. 1(a). For benzene molecule [2] SERS surface selection rule states that vibrational bands which draw the intensity of Raman polarizability component  $\alpha_{zz}$  is the most intense, where  $z$  is the surface normal. If a benzene molecule is adsorbed, such that the ring lies parallel to the metal surface,  $\alpha_{zz}$  contributes only to its two  $A_{1g}$  modes  $v_1$  (at 992  $\text{cm}^{-1}$ ) and  $v_2$  (at 3056  $\text{cm}^{-1}$ ). The maximum contribution to the  $\alpha_{zz}$  component of the polarizability of benzene comes from the  $\pi$ -electrons. Thus,  $v_1$ , which perturbs the carbon ring directly, plays a more prominent role in affecting  $\alpha_{zz}$  than  $v_2$ , which involves only hydrogen atoms [2]. However, if the benzene ring is perpendicular to the metal surface rather than lying parallel, one expects  $v_2$  would be more intense than  $v_1$ . In aqueous Phe these two peaks of the aromatic ring structure appear at 1008 and 3080  $\text{cm}^{-1}$ . In SERS spectra these modes are obtained at 1000 (shown by ★ in Fig. 6) and 3065  $\text{cm}^{-1}$  (as X in the same figure). Above the pH value 3.5, the intensity of the band at 1000  $\text{cm}^{-1}$  increases with increase in pH of Phe till the pH value reaches 9.5. Beyond this value of pH the 1000  $\text{cm}^{-1}$  band disappears [Fig. 7a]. The intensity ratio of the peak at 1008  $\text{cm}^{-1}$  to that at 3080  $\text{cm}^{-1}$  for Phe–C is 3.4 (Fig. 5). However the value of the ratio for the corresponding peaks in the SERS spectra increases from 3.1 to 5.5 with increase in pH. The higher intensity ratio in SERS spectra compared to what we have observed for Phe–C indicates that with increase in pH there is a conformational change in the molecule; the attached molecule tilts more and more towards the surface (flatter) as indicated by the increase

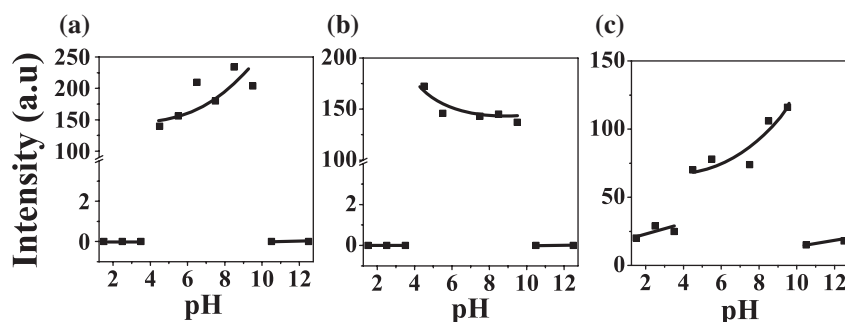


Fig. 8. Intensity variation of SERS bands at (a) 1375, (b) 1582 and (c) 1036  $\text{cm}^{-1}$  with pH variation from 1.5 to 12.5 for Phe–Ag complex.

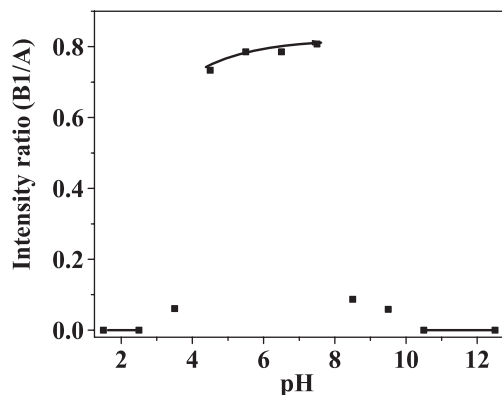


Fig. 10. Variation of intensity ratio of peak B1 and peak A in optical absorption spectra for Tyr-Ag complex.

in ratio of  $I(\nu_1)/I(\nu_2)$ , shown in Fig. 7(b). The above intensity variation and shift in the frequency of these bands in the SERS spectrum with respect to their frequencies in the Raman spectrum of the solution indicate that the  $\pi$ -system of Phe participates in complex formation with Ag.

In Fig. 6, a relatively strong band at  $1375\text{ cm}^{-1}$  (marked by \$ in Fig. 6) beyond pH value 3.5 (note that  $pK_1=2.58$  for Phe) and the variation in intensity of this band with pH indicate that the carboxylic group,  $-\text{COO}^-$ , upon deprotonation is clearly adsorbed on the surface of the Ag colloids [Fig. 8(a)]. There are several weak bands between  $500$  and  $750\text{ cm}^{-1}$  due to different  $\text{COO}^-$  vibrational modes. In SERS spectra of Phe-Ag the CH-stretching vibration appears at  $2915\text{ cm}^{-1}$ . The  $\nu\text{CH}_2$  vibrational modes are absent in SERS spectra, indicating that the methylene group is relatively far from the Ag surface. Though, it is not expected that the  $\text{NH}_3^+$  group be directly attached to  $\text{Ag}^+$  colloids in the sol, the relatively strong band due to asymmetrical deformation of  $\text{NH}_3^+$  at  $1582\text{ cm}^{-1}$  (as + in Fig. 6) indicates that the amine group of the molecule stays relatively close to the Ag surface. The intensity of this band decreases with increase in pH as  $\text{NH}_3^+$  transforms to  $\text{NH}_2$  [Fig. 8(b)]. The relatively strong band due to  $\nu\text{CN}$  at  $1036\text{ cm}^{-1}$ , and its increase in intensity with increase in pH [Fig. 8(c)], can be explained by assuming the proximity of the amine group to the silver surface.

### 3.2. Tyrosine (Tyr): results and discussion

The optical absorption spectra of Tyr at different pH in colloidal solution of Ag are shown in Fig. 9. As observed in case of Phe [Fig. 2], the addition of Tyr to the sol results in the appearance of a new band at around  $500\text{ nm}$  (B1) due to

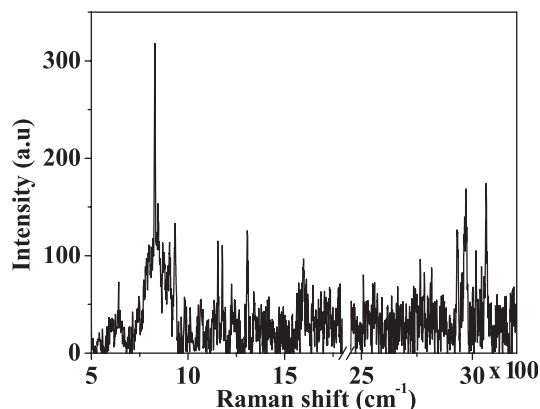


Fig. 12. Raman spectrum of Tyr in solution at concentration 0.5 M.

aggregation of Ag sol along with a decrease in intensity of peak A (due to the Ag colloids without adsorbate). The variation in the ratio of the intensity of peak B1 to that of peak A with change in pH is shown in Fig. 10. The nature of aggregation of the silver particles with addition of Tyr of different pH, as obtained from TEM images, are shown in Fig. 11(a)–(c).

In Fig. 12 we have shown the Raman spectrum of an aqueous Tyr solution of 0.5 M (Tyr-C) at pH 6.0 after subtracting the luminescence background. It is to be noted that the signal to noise ratio ( $S/N$  ratio) in the observed Raman spectrum is small. Increasing acquisition time is usually an option for improving the  $S/N$  ratio. However, in our experiment, such an increased acquisition time is not a viable solution since it increases the intensity of the luminescence background, thereby masking the Raman signal completely. With the help of reported Raman lines for Tyr [9], we have assigned vibrational bands in Tyr-C to different modes, which has been summarized in Table 2. The most intense band at  $828\text{ cm}^{-1}$  has been assigned to the breathing mode of the aromatic ring structure of Tyr [9]. Other less intense but prominent bands, appear at  $931$ ,  $1304$  and  $2967\text{ cm}^{-1}$ , are due to  $\text{C}-\text{COO}^-$ ,  $\text{CH}_2$  wagging and  $\text{CH}$  vibrations, respectively. The bands belonging to  $\nu\text{CH}$  vibrations in the ring appear at  $3061\text{ cm}^{-1}$ .

The SERS spectra of Tyr ( $1 \times 10^{-3}\text{ M}$ ) with pH from 1.5 to 12.5 are shown in Fig. 13. Raman spectrum of aqueous Tyr solution of same concentration at pH 7 is shown by a dotted line in the same figure. It is interesting to note that though the molecular structure of Tyr is similar to that of Phe except for an  $-\text{OH}$  group in the *para* position of the aromatic ring, the SERS spectrum is entirely different from that of Phe. In aqueous solution, Tyr becomes Tyrosinate,  $\text{TyrO}^-$ , at pH of

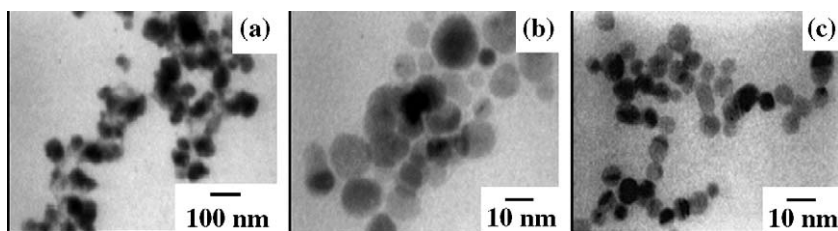


Fig. 11. Transmission electron micrograph of Tyr-Ag mixture at (a) pH 2, (b) pH 7.5, and (c) pH 11.

Table 2

Assignment of vibrational bands for Tyr-C Raman spectrum

Assignment	Tyr-C ( $\text{cm}^{-1}$ )
Ring breathing mode	828
C–COO <sup>−</sup>	931
CH <sub>2</sub> wagging	1304
CH	2967
CH vib. in ring	3061

10.07 (pK<sub>3</sub>). However, Tyr deprotonates upon adsorption, i.e. they are adsorbed as TyrO<sup>−</sup> on metal surface (it has been shown that SERS spectra of Tyr–Ag should cover much narrower spectral region) [3,9]. We assign the broad and unresolved band envelope between 1200 and 1500  $\text{cm}^{-1}$  in Fig. 13, measured with long integration time (2 min as in our case) for the range of pH value from 3.5 to 9.5, to temporal averaging (averaging of strongly fluctuating contribution to overall intensity profile) of Tyr SERS spectrum. The reason is the following: in addition to the direct coordination of the aromatic ring with Ag<sup>+</sup>, TyrO<sup>−</sup> can be adsorbed on the Ag surface either via the carboxylic acid group or via both the amino and carboxylic group or via the phenol hydroxyl group. The ensemble average of all these complexations results in a broad band. This has also been shown from quantum chemical estimates of vibrational energies using Hartree–Fock self-consistent field molecular orbital calculation for TyrO<sup>−</sup>–Ag complex [3]. In Fig. 14 we have shown the variation in the intensity of the peak at 1390  $\text{cm}^{-1}$  with the pH of the Tyr solution. In the acidic region (pH < 4.5) an extensive aggregation and subsequent precipitation of the colloidal silver lead to a complete loss of the SERS signal. The decrease in SERS spectral intensity for higher pH at 10.5 and above is due to spreading out of the Ag particles in the sol, which decreases the number of hot sites necessary for SERS [Fig. 11 (c)]. Following the discussion on Phe–Ag complex, the role of agglomeration of Ag particles (formation of the number of hot sites in metal sol) to exhibit efficient SERS of Tyr–Ag complex is also clear from the variation in intensity ratio of peak B1 and peak A with pH in absorption spectra as shown in Fig. 10 and also from the TEM images shown in Fig. 11.

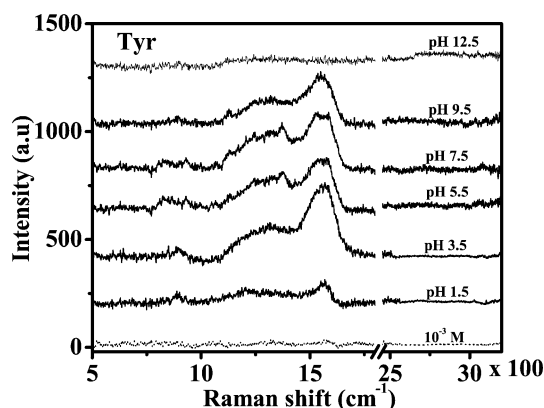


Fig. 13. Raman spectrum of Tyr (dotted) and SERS spectra (solid lines) of Tyr–Ag complex ( $1 \times 10^{-3}$  M) at different pH.

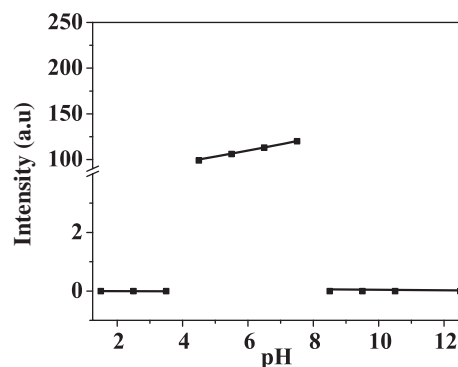


Fig. 14. Intensity variation of Raman bands at 1390  $\text{cm}^{-1}$  in Tyr with change in pH from 1.5 to 12.5.

### 3.3. Comparison of interaction in Phe–Ag and Tyr–Ag complex

From the above experimental results and the corresponding discussion we observe that the Phe and Tyr molecules behave very differently while forming complexes with Ag molecules. For Phe the aromatic ring lies nearly flat on Ag surface. Both carboxylic and amine groups are important in adsorption of Phe on metal particles; whereas, the methylene (CH<sub>2</sub>) group is relatively inert. This signifies that the aromatic ring, carboxylic and amine group of Phe lie in close proximity of metal particles, whereas the methylene group stays away. On the other hand, Tyr adsorbs on Ag surface as Tyrosinate. At any instant of time, interaction of metal ion either with carboxylic group or with amine group or with oxygen in the side chain can be more probable than the other two interactions.

To support our above conjecture, we have looked into the atomic charge distribution at the different terminals of Phe and Tyr molecules in the energy minimized zwitterionic forms (which bind with Ag ion to form a complex), shown in Fig. 15(a) and (b). From the hybrid density functional theory, it has been shown that while forming a complexes with Phe or Tyr, the Ag<sup>+</sup> preferentially occupies the cavity formed in the molecular structure, shown in Fig. 15 [13]. If one takes into account only the electrostatic affinity between Ag and Phe/Tyr molecule, from the atomic charge distribution, shown in Fig. 15, it appears that the following interactions are possible for both Ag–Phe or Ag–Tyr complexes — (a) it is unlikely for the NH<sub>3</sub><sup>+</sup> group to be directly attached with the positively charged Ag surface, though it is in close proximity of the Ag<sup>+</sup>; (b) the CH<sub>2</sub> group is away from Ag<sup>+</sup>, which results in a weak electrostatic interaction between them; (c) the negative charge distribution on oxygen atoms of the carboxylic acid group and ring structure indicate the possibility of a strong electrostatic interaction with the positive metal ion; and (d) the aromatic ring is parallel to the surface of the Ag<sup>+</sup>. From a more careful analysis we see that in Phe the charges on the oxygen atoms of the carboxylic group are −0.56 units, whereas, those on Tyr are −0.29 and −0.36 units. The side chain oxygen atom of Tyr has a charge of −0.34 units. We believe the relatively large negative charge on oxygen terminals in Phe holds the positive metal ion firm in its position via Coulombic interactions.

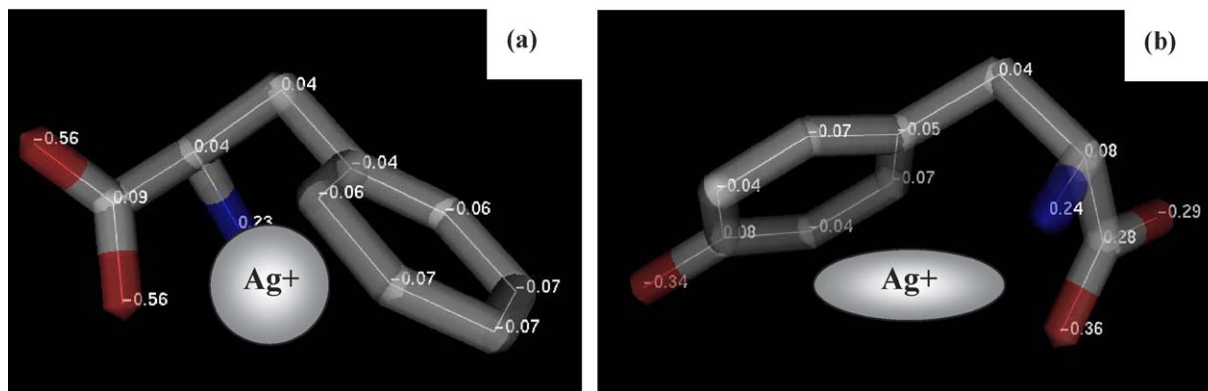


Fig. 15. Atomic charge distribution on (a) Phe and (b) Tyrosinate, obtained by Gasteiger–Hückel method.

However, the relatively weaker negative charges at the carboxylic oxygen terminals and at the side chain result in a smeared position of the  $\text{Ag}^+$  in the Tyr cavity [Fig. 15 (b)] compared to what we observe in case of the Phe–Ag complex [Fig. 15 (a)]. This explains the weak and broad SERS band for Tyr–Ag complex. It is also interesting to note that except in these terminals, the charge distributions are nearly the same on all other atoms in Phe and Tyr.

#### 4. Kinetic measurements on Ag–Phe and Ag–Tyr interaction

We have seen in the previous section that the formation of hot sites due to the optimum agglomeration of Ag colloidal particles plays a direct role in forming stable Ag–ligand complexes. In this section, we have confirmed the same fact by measuring the interaction kinetics of Phe–Ag and Tyr–Ag complexes by SERS and absorption measurements. To study the kinetics of the interaction we have recorded the intensity of optical absorption peak at 550 nm (peak B due to agglomerated

Ag in Fig. 2) for Phe–Ag complex and 500 nm (peak B1 in Fig. 9) for Tyr–Ag complex with time. The variations in intensities of these two peaks with time are shown in Fig. 16(a) and (b), respectively. We clearly observe two different decay rates for both the peaks. For the first 120 s the decay process is very fast compared to what is observed later. The decay time constants are 58 ( $\tau_1$ ) s and 178 ( $\tau_2$ ) s for Phe and 63 ( $\tau_1$ ) s and 100 ( $\tau_2$ ) s for Tyr.

To correlate the optical absorption and SERS measurements, we studied the kinetics of SERS spectra of  $5 \times 10^{-3}$  M ligand–Ag mixture at pH 8 (about which we get maximum SERS intensity for the most intense peaks). Each spectrum was taken for 1 min. The exponential drop in intensities of the strongest band at  $1000 \text{ cm}^{-1}$  for Phe and the band at  $1390 \text{ cm}^{-1}$  in Tyr are shown in Fig. 17(a) and (b). The decay constants are estimated to be 213 and 113 s, respectively. These values of the time constants match reasonably well with the values of  $\tau_2$ , which we have obtained from optical absorption measurements. Thus, we confirm that the metal–amino acid interaction is directly related to the aggregation of the Ag colloids. Here we would like to mention that because of experimental limitations the absorption spectra in Figs. 2

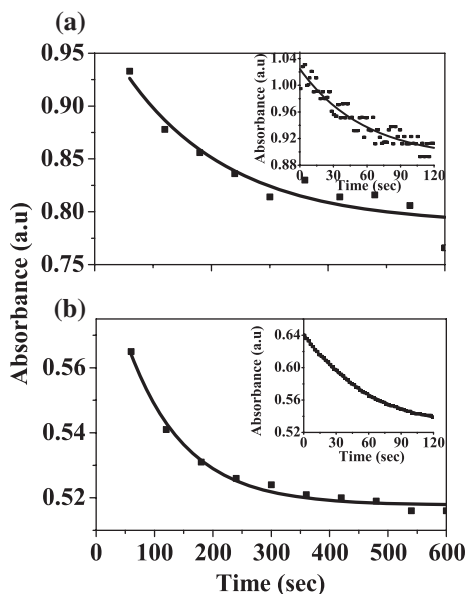


Fig. 16. Kinetic study of (a) the feature at 550 nm in optical absorption spectra of Phe–Ag mixture and (b) the feature at 500 nm for Tyr–Ag complex. Insets of the figures show the same for the first 2 min duration.

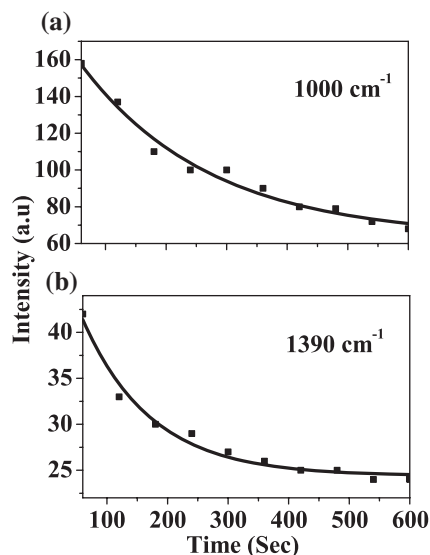


Fig. 17. Kinetic study of the most intense peak in SERS spectra for (a) Phe–Ag complex and (b) Tyr–Ag complex.



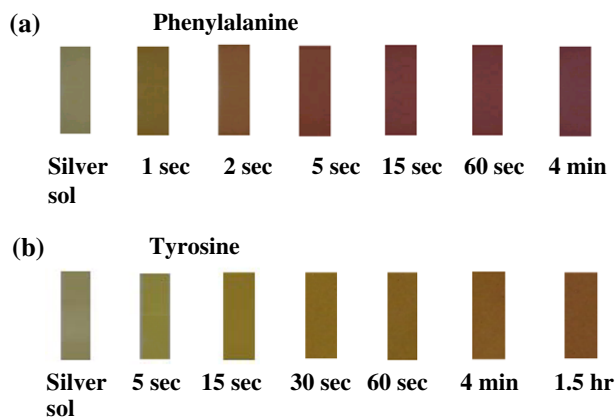


Fig. 18. Change in colour of (a) Phe–Ag complex and (b) Tyr–Ag complex with time.

and 9 or SERS spectra in Figs. 6 and 13 are recorded 2 min after addition of amino acids in Ag sol. Thus, the effect of initial kinetics of interaction, at time scale  $\tau_1$ , is not observed in these spectra.

However, a careful observation of the initial change in colour of the sol with addition of amino acid indicates fast kinetics of the interaction between ligand molecules and Ag sol. The as-prepared Ag sol is yellow in colour and is stable for more than 24 h at 4 °C. The agglomeration of the particle after addition of amino acids changes the colour from yellow to pink to blood red as shown in Fig. 18(a) for Phe and yellow to amber to olive green as shown in Fig. 18(b) for Tyr. It is to be noted that the change in colouration of the solution is rapid (distinct by naked eye) for first  $\sim 60$  s for both Phe–Ag and Tyr–Ag. This time scale matches with the value of  $\tau_1$  obtained from kinetic studies by absorption measurements. This initial change in colour may be due to the increase in the size of the particles from single particle to doublets, triplets and higher multiplets. Gradually, with time, the colour of the solution fades out indicating the breakdown of agglomerated particles into smaller fragments.

## 5. Summary

Though structurally close, Phe and Tyr, behave very differently, when they form complexes with Ag colloids. To understand this difference, we have compared the metal–amino acid interaction in Phe–Ag and Tyr–Ag complexes by pH dependent SERS measurements. From the intensity variations of the vibrational bands in SERS spectra with the pH of the adsorbates, we have proposed the relative orientation and interaction of the adsorbed molecules on the Ag surface. We have addressed a long standing query, as to whether the amine group is directly attached with Ag surface along with carboxylate group in these systems.

Using Gasteiger–Hückel method to estimate the atomic charge distribution at different terminals of the zwitterionic amino acid molecules, we have noted that, though the structures of Phe and Tyr are quite similar, except an –OH group at the *para* position of the ring in the latter, the atomic

charge distributions at the oxygen sites of these molecules, are quite different. If we assume only the electrostatic interaction between different terminals of the adsorbates with  $\text{Ag}^+$ , the above charge distribution confirms the interaction and orientation of the amino acid molecules in the complexes, which we have proposed from SERS measurements.

In addition, the appearance of SERS bands has been explained with the help of pH dependent TEM and optical absorption measurements. We have seen that the pH values of the amino acid–Ag sol show an appreciable change in comparison with the values for the initial amino acid solution, only when the ligand molecules are in zwitterionic form. This implies that there is a favorable interaction of the added molecules of this form to the Ag clusters in the sol. This result is finally confirmed by the intensity variation of the SERS and optical absorption spectra of Phe–Ag and Tyr–Ag complexes and also substantiated by the TEM images taken at different pH. We have seen that the formation of hot sites via optimum aggregation of Ag particles induced by Phe/Tyr results in an increase in intensity of the optical absorption band of the Ag aggregates and, concurrently, an increase in SERS band intensities. We have also shown that the state of aggregation is a key parameter in SERS. We have discussed the reaction kinetics of this interaction process using spectroscopic measurements.

## Acknowledgements

Authors thank P.V. Satyam and J. Ghatak, IOP, Bhubaneswar, India, for their assistance in the TEM work. The authors would also like to express their gratitude to a reviewer for helpful suggestions. AR thanks Department of Science and Technology, India, and Third World Academy of Science, ICTP, Italy for financial assistance.

## References

- [1] T. Shoeib, A. Cunje, A.C. Hopkinson, K.W. Michkael Siu, Gas-phase fragmentation of the  $\text{Ag}^+$ –Phenylalanine complex: cation —  $\pi$  interactions and radical cation formation, *J. Am. Soc. Mass Spectrom.* 13 (2002) 408–416.
- [2] J.S. Suh, M. Moskovits, Surface-enhanced Raman spectroscopy of amino acids and nucleotide bases adsorbed on silver, *J. Am. Chem. Soc.* 108 (1986) 4711–4718.
- [3] E.J. Bjerneld, P. Johansson, M. Kall, Single molecule vibrational fine-structure of tyrosine adsorbed on Ag nanocrystals, *Single Mol.* 3 (2000) 239–248.
- [4] E.J. Bjerneld, F. Svedberg, P. Johansson, M. Kall, Direct observation of heterogeneous photochemistry on aggregated Ag nanocrystals using Raman spectroscopy: the case of photoinduced degradation of aromatic amino acids, *J. Phys. Chem., A* 108 (2004) 4187–4193.
- [5] D. Curley, O. Siiman, Conformation and orientation of the haptens, 2,4-Dinitrophenyl amino acids, on colloidal silver from surface-enhanced Raman scattering, *Langmuir* 4 (1988) 1021–1032.
- [6] K. Kneipp, H. Kneipp, I. Itzkan, R.R. Dasari, M.S. Feld, Ultrasensitive chemical analysis by Raman spectroscopy, *Chem. Rev.* 99 (1999) 2957–2975.
- [7] B. Teiten, A. Bumeau, Detection and sorption study of Dioxouranium (VI) ions on *N*-(2-Mercaptopropionyl) glycine-modified silver colloid by Surface enhanced Raman scattering, *J. Raman Spectrosc.* 28 (1997) 879–884.

- [8] It is generally agreed that there is more than one factor which results in SERS. The most important factors are (i) the effect of electromagnetic field and (ii) chemical first-layer effect. The latter effect includes enhancement due to specific interaction (electronic coupling) between metal and molecules. Electronic SERS occurs due to metal–molecule charge-transfer electronic transitions. The effect of chemical enhancement is less than that of electronic enhancement. For more detail one can look into Ref. [6].
- [9] R.P. Rava, T.G. Spiro, Selective enhancement of Tyrosine and Tryptophan resonance Raman spectra via ultraviolet laser excitation, *J. Am. Chem. Soc.* 106 (1984) 4062–4064;  
F. Ota, S. Higuchi, Y. Gohshi, K. Furuya, M. Ban, M. Kyoto, Some considerations of the SERS effect of L-Phenylalanine in the near-infrared region using silver colloid solution, *J. Raman Spectrosc.* 28 (1997) 849–854.
- [10] J. Creighton, C. Blatchford, M. Albrecht, Plasma resonance enhancement of Raman scattering by Pyridine adsorbed on silver and gold sol particles of size comparable to the excitation wavelength, *J. Chem. Soc., Faraday Trans.* 75 (1979) 790.
- [11] S.P.A. Fodor, R.A. Copeland, C.A. Grygon, T.G. Spiro, Deep-ultraviolet Raman excitation profiles and vibronic scattering mechanisms of phenylalanine, tyrosine and tryptophan, *J. Am. Chem. Soc.* 111 (1989) 5509–5518.
- [12] R.P. Rava, T.G. Spiro, Resonance enhancement in the ultraviolet Raman spectra of aromatic amino acid, *J. Phys. Chem.* 89 (1985) 1856–1861.
- [13] T. Shoeib, K.W. Michael Siu, A.C. Hopkinson, Silver ion binding energies of amino acids: use of theory to assess the validity of experimental silver ion basicities obtained from the kinetic method, *J. Phys. Chem.* 106 (2002) 6121–6128.